A-DEPENDENCE IN PHOTOPRODUCED JETS

Donna Naples
University of Maryland
presented for FNAL E683 collaboration

Abstract

Fermilab E683 studied high p_T jets produced by a high energy real photon beam impinging on hydrogen, deuterium, and six nuclear targets. The tagged photon beam energies ranged from 50 to 400 GeV. Data were collected with a segmented large acceptance calorimeter. Jets with p_T in the range 3-7 GeV/c were reconstructed. Measurements of a component of the transverse momentum imbalance, $k_{t\phi}$, as a function of atomic weight will be presented. Data were also taken with a broad band pion beam at the same mean $\sqrt{s}$ ($\sim$ 21.5 GeV) and will be compared with the photoproduction data. We also present a comparison of the A-dependence behavior at different beam energies.

Nuclear dependence has long been seen at high p_T in jet and single particle production from hadron-nucleus collisions [1]. A-dependence in jet production from photon-nucleus interactions has not been studied before. The generally accepted interpretation of the A-dependence is rescattering of partons as they traverse the nuclear medium in which the hard interaction has taken place. Recent approaches to the problem have attempted to predict the A-dependence using non-leading power contributions in perturbative QCD [2].

Here we present a study of nuclear dependence of the variable $k_{t\phi}$ for both photon-nucleus and pion-nucleus high p_T interactions. The variable $k_{t\phi}$ (defined below) is the out-of-plane component of the net transverse momentum of the di-jet system. Most previous observations of nuclear dependence report the behavior of the cross section at fixed high p_T as a function of atomic weight [1]. The kinematic variable $k_{t\phi}$ is more directly sensitive to the effects of multiple scattering. The relation of $k_{t\phi}$ and α has been discussed in reference [3].

Experiment 683 was performed in the Wide Band beamline at Fermilab during the 1991 fixed target run. The tagged photon beam energies ranged from 50 to 400 GeV. About 10% of our data was taken with a broad band pion beam. The triggered mean energy of both beam types was about 250 GeV. The targets studied include hydrogen, deuterium, Be, C, Al, Cu, Sn, and Pb.

The main component of the E683 detector used in this analysis was the highly segmented, wide angle calorimeter (MCAL). The MCAL has full azimuthal acceptance and a polar angle acceptance in the γp center of mass of $25° < \theta^* < 100°$ at $\sqrt{s} = 21$ GeV. The MCAL face is segmented into 132 towers each subtending $\Delta\eta \simeq 0.18$ and $\Delta\phi \simeq 0.26$ rads. The MCAL resolution is estimated to be on the order of $35\%/\sqrt{E}$ for electromagnetic energy and $85\%/\sqrt{E} \oplus 10\%$ for hadronic energy (where '$\oplus$' symbolizes addition in quadrature).

The MCAL was the basis for our high E_t discrimination trigger. We used two types of di-jet triggers concurrently. The TWOHI trigger required at least two MCAL towers to have transverse energy, E_t, greater than about 0.5 GeV each. The GLOBAL trigger required a minimum total E_t in the MCAL of about 7 GeV. Events were selected with either GLOBAL $E_t > 8$ GeV or TWOHI $E_t > 0.75$ GeV to remove hardware inefficiencies near the thresholds for each trigger. Additional 'fake' high E_t triggers in our detector could come from δ-ray production or bremsstrahlung by beam line halo muons at wide angles or phototube breakdown in the MCAL itself. These events had low total energy and multiplicity and were easily cut out of our data sample.

Jets in the p_T range 3-7 GeV/c were reconstructed by applying a standard (η, ϕ) cone jetfinding algorithm with cone radius of $R = 1.0$ to the data. Di-jets events were required to have each jet $p_T \geq 3$ GeV/c. Also, the polar angle of the jet axis in the lab frame was restricted between $2° < \theta_{\rm LAB} < 6°$ to insure jet containment in the calorimeter. A correction was applied for the non-target related events of between 10 and 20% depending on the target.

We define the $k_{t\phi}$ for a di-jet event using the plane defined by the beam direction and the momentum vector of the higher p_T jet to be the component of k_t out of the plane:

$$k_{t\phi} = P_T \sin(\Delta\phi),$$

where P_T is the average jet p_T of the event and $\Delta\phi$ is the azimuthal opening angle between the jets. All plots of $k_{t\phi}$ show the RMS value of the $k_{t\phi}$ distribution.

Figure 1a plots the RMS value of $k_{t\phi}$ as a function of atomic weight for both photon-nucleus and pion-nucleus data. There is a clear A-dependence in both cases. The normalized target empty $k_{t\phi}$ distribution was subtracted bin-by-bin from each target's $k_{t\phi}$ distribution. There is a significant offset in the two data sets which will be discussed further. We will assume three uncorrelated contributions to $k_{t\phi}$ in this analysis. Contributions are expected from: (i) gluon radiation and intrinsic parton Fermi motion within the nucleon, (ii) jetfinding and calorimetry in our measurement, and (iii) nuclear contributions (for A¿1).

We will first discuss the calorimetry and jetfinding contributions to the measurement and correct for them. The energy resolution, shower spreading, and granularity of the MCAL all add width to the $k_{t\phi}$ distribution. Particle inclusion errors in jetfinding will smear the found jet p_T's and angles and will therefore add a width to the $k_{t\phi}$ distribution. Jetfinding is particularly sensitive to the non-jet E_t from the underlying event at these low jet p_T's. There is evidence for more underlying event in the jet events produced with pions as compared with those from photoproduction. Shown in figure 2a is the average non-jet E_t, which is the total E_t outside of the jet cones in a di-jet event, as a function of jet p_T. The non-jet E_t is on the order of 30% higher in the pion-proton jet events. Figure 2b plots the E_t per 3° bin in azimuthal angle from the hotter jet's axis per event. The underlying event in the pion-produced events is clearly larger than in photoproduced events.

Our measurement was corrected for these effects by using a Monte Carlo study. Events were simulated in our MCAL detector and the jetfinding algorithm was then applied to the simulated calorimeter towers. The vector sum of the momenta of the particles originating from each hard scatter parton defines the 'true' jet. The correction was obtained by quadrature subtraction of the ensemble value of $k_{t\phi}$ of the 'true' jet distribution from that of the reconstructed jets.

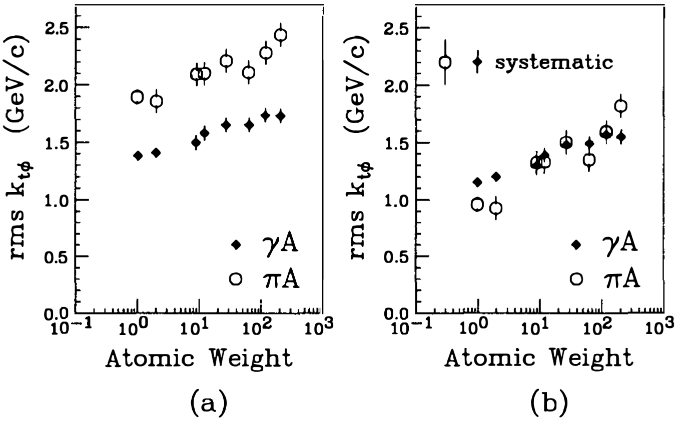

Figure 1: RMS value of $k_{t\phi}$ (a single component of the transverse momentum unbalance in the di-jet system) as a function of atomic weight for γA and πA . a.) uncorrected data b.) after jetfinding contributions are removed.

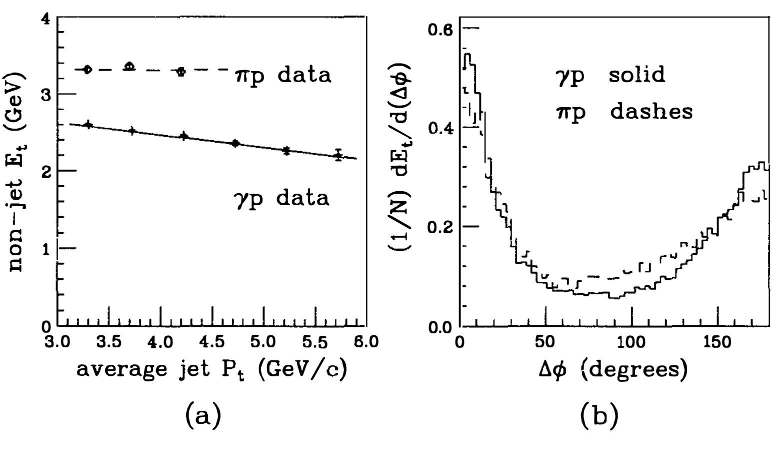

Figure 2: a.) E_t outside of the jet cones. b.) E_t flow per event for pion-proton events (dashes) and photon-proton events (solid).

For the photon-proton case we used a mixture of the LUND Monte Carlos, LUCIFER and TWISTER [6] (with JETSET 6.3) with Field-Feynman independent fragmentation as an event generator to model our data. We have demonstrated that this is a good representation of our photoproduced event structure [4]. To model our pion-proton data adequately we included extra underlying event in the Monte Carlo. The parameterization of the underlying event used was extracted from HERWIG [5] Monte Carlo. The correction to the RMS value of $k_{t\phi}$ for γp was 0.75 ± 0.1 GeV. For πp the correction was 1.6 ± 0.3 GeV. The systematic uncertainty takes into account the modeling of the underlying event contribution. The corrected data is shown in figure 1b. The two data sets now lie on top of each other.

In subtracting the same value for the jetfinding correction from each target we implicitly assumed that it was independent of A. The jetfinding correction is dominated by the underlying event particle inclusion errors. We have checked that the underlying event is not A-dependent. It was found that the non-jet E_t fraction, the ratio of the E_t outside of the jet cone to the total E_t in the event, does not vary with A for either photon-nucleus or pion-nucleus events.

The nuclear contribution to $k_{t\phi}$ is shown for both data sets in figure . It is obtained by subtracting the RMS $k_{t\phi}$ value at A=1 from that for each nuclear target in quadrature. The curves are fitted with linear fits for comparison of the slope. The solid line fits include all the data points and the dashed lines are fits to only the targets with A> 2. The slopes of the linear fits are 0.50 ($\pm$ 0.04) (solid) and 0.27 ($\pm$ 0.11) (dash) for photon data; and 0.67 ($\pm$ 0.07) (solid) and 0.42 ($\pm$ 0.23) (dash) for pion data. Both beam types see a comparable A-dependence (the pion-nucleus data may be slightly stronger).

Because we had a broad band beam we were able to extract the behavior of the A-dependence with photon beam energy. This is shown in figure 4 where the RMS value of $k_{t\phi}$ is plotted as a function of A for three different energy bins. Some of the targets with similar atomic weights were grouped together to improve statistics (Be+C, Al+Cu, and Sn+Pb). The slope of $k_{t\phi}$ versus A appears to increase with energy for the three energy bins studied. There is also an offset in the curves which increases with energy. This is likely due to an energy dependent contribution to the underlying event however we might also expect gluon radiation contributions in $k_{t\phi}$ to increase with energy. An understanding of the behavior of the A-dependence with energy may lead to a better understanding of the mechanism.

In conclusion, we have measured a clear A-dependence in $k_{t\phi}$ from photoproduced jets. It is comparable with that seen in our pion-produced jet sample taken at the same $\sqrt{s}$. The A-dependence appears to increase with energy. In addition, there appears to be less underlying

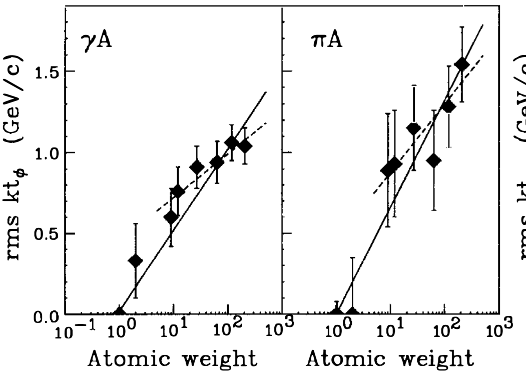

Figure 3: Nuclear contribution to k_{t_ϕ}.

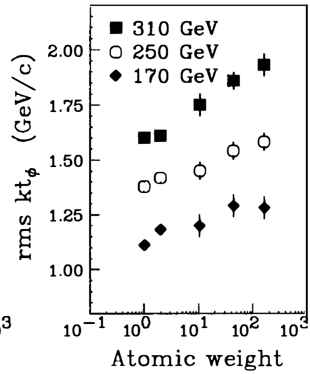

Figure 4: A–dependence of k_{t_ϕ} for three energy bins.

event present in γp collisions than in πp collisions at the same $\sqrt{s}$.

References

[1] J. Cronin et al., Phys. Rev. Lett. **31** 1426 (1973); C. Bromberg et al., Phys. Rev. Lett. **42** 1202 (1979); Brown et al., Phys. Rev. Lett. **50** 11 (1983); M. Corcoran et al., Phys. Lett. **B259** 209 (1991).

[2] M. Luo, J. Qui, and G. Sterman, Phys. Lett. **B279** 377 (1992).

[3] T. Fields, Nucl. Phys **A544** 565 (1992); T. Fields and M. Corcoran, Phys. Rev. Lett. **70** 143 (1993).

[4] D. Adams et al., Rice University preprint *DE/F605/92ER40717-6* (May 1993).

[5] Marchesini and Webber, Comp. Phys. Comm. **67** 465 (1992).

[6] G. Ingelman and A. Weigand, Comp. Phys. Comm. **46** 241 (1987); G. Ingelman and A. Weigand, Comp. Phys. Comm. **46** 217 (1987); T. Sjostrand, Comp. Phys. Comm. **43** (1987) 367.